Journal of Modern Physics, 2017, 8, 1749-1761
http://www.scirp.org/journal/jmp
ISSN Online: 2153-120X
ISSN Print: 2153-1196

NO_2 Excited State Properties Revisited: An Effect of Extra Compactified Dimensions

Hans-Georg Weber[1,2]

[1]Heinrich-Hertz-Institut, Einsteinufer 37, Berlin, Germany
[2]Sudetenstr. 16, Amorbach, Germany
Email: hans-georg.weber@gmx.de

How to cite this paper: Weber, H. G. (2017) NO_2 Excited State Properties Revisited: An Effect of Extra Compactified Dimensions. *Journal of Modern Physics*, **8**, 1749-1761.
https://doi.org/10.4236/jmp.2017.811103

Received: September 2, 2017
Accepted: October 7, 2017
Published: October 10, 2017

Abstract

Experiments on NO_2 reveal a substructure underlying the optically excited isolated hyperfine structure (hfs) levels of the molecule. This substructure is seen in a change of the symmetry of the excited molecule and is represented by the two "states" $|b\rangle$ and $|c\rangle$ of a hfs-level. Optical excitation induces a transition from the ground state $|a\rangle$ of the molecule to the excited state $|b\rangle$. However, the molecule evolves from $|b\rangle$ to $|c\rangle$ in a time $\tau_0 \approx 3$ µs. Both $|b\rangle$ and $|c\rangle$ have the radiative lifetime $\tau_R \approx 40$ µs, but $|b\rangle$ and $|c\rangle$ differ in the degree of polarization of the fluorescence light. Zeeman coherence in the magnetic sublevels is conserved in the transition $|b\rangle \to |c\rangle$, and optical coherence of $|a\rangle$ and $|b\rangle$ is able to affect (inversion effect) the transition $|b\rangle \to |c\rangle$. This substructure, which is not caused by collisions with baryonic matter or by intramolecular dynamics in the molecule, contradicts our knowledge on an isolated hfs-level. We describe the experimental results using the assumption of extra dimensions with a compactification space of the size of the molecule, in which dark matter affects the nuclei by gravity. In $|a\rangle$, all nuclei of NO_2 are confined in a single compactification space, and in $|c\rangle$, the two O nuclei of NO_2 are in two different compactification spaces. Whereas $|a\rangle$ and $|c\rangle$ represent stable configurations of the nuclei, $|b\rangle$ represents an unstable configuration because the vibrational motion in $|b\rangle$ shifts one of the two O nuclei periodically off the common compactification space, enabling dark matter interaction to stimulate the transition $|b\rangle \to |c\rangle$ with the rate $(\tau_0)^{-1}$. We revisit experimental results, which were not understood before, and we give a consistent description of these results based on the above assumption.

Keywords

Extra Dimensions, Compactification Space, Dark Matter, Molecular Physics

1. Introduction

Various experiments on NO_2 reveal two characteristic time constants associated with the optically excited hyperfine structure (hfs) levels of the molecule, the radiative decay time $\tau_R \approx 40$ μs and the time constant $\tau_0 \approx 3$ μs, which is no radiative decay time, not caused by collisions with baryonic matter, and not caused by intramolecular dynamics in the molecule [1] [2]. For example, optical excitation of NO_2 in a molecular beam near the excitation wavelength $\lambda_{ex} = 593$ nm induces a transition between a state $|a\rangle$ of the ground electronic state (X^2A_1) and a state $|b\rangle$ of the first excited electronic state (A^2B_2). However, the state $|b\rangle$ is not stable [1] [2]. The isolated molecule evolves in a radiationless and irreversible process from $|b\rangle$ to a state $|c\rangle$ in a time $\tau_0 \approx 3$ μs, which is short compared to the radiative lifetime $\tau_R \approx 40$ μs of both $|b\rangle$ and $|c\rangle$ [1] [2], but long compared to the time domain of intramolecular dynamics in NO_2 (e.g. [3] [4]). The two states $|b\rangle$ and $|c\rangle$ have the same radiative lifetime but differ in the degree of polarization of fluorescence light [1] [2]. The transition $|b\rangle \to |c\rangle$ is smooth. Zeeman coherence in the magnetic sublevels is conserved in the evolution of $|b\rangle$ to $|c\rangle$. The experiments in Refs. [1] [2] were using magnetic field induced depolarization of the fluorescence light (zero-magnetic field level-crossing or Hanle effect measurement) as well as optical radio-frequency double resonance. These experiments give τ_0 and τ_R as coherence decay times. The lifetime τ_R is in agreement with results of radiative decay measurements revealing single-exponential decay ([5] and references given there).

The transition $|b\rangle \to |c\rangle$ exhibits an unusual feature, named inversion effect, which was not seen on atoms and molecules before ([1] [2] and references given there). The inversion effect is an inversion of the distribution of the occupation probabilities c_m of the magnetic sublevels $|c,m\rangle$ of $|c\rangle$ versus the light intensity I or versus the transit time T_L of the molecules through the light beam. Optical coherence (e.g. $\Delta m = 0$ for π excitation) reduces the decay rate of $|b,m\rangle$ to $|c,m\rangle$ by the coupling of $|b,m\rangle$ to the ground state $|a,m\rangle$. The occupation probabilities are $b_m \sim Z_m(1+Z_m)^{-1}$ for $|b,m\rangle$ and $c_m \sim Z_m(1+Z_m)^{-2}$ for $|c,m\rangle$ with $Z_m = \tau_0 T_L (2v_m)^2$, where $2v_m$ is the Rabi frequency. This gives $c_m \sim Z_m$ for low values of IT_L and $c_m \sim (Z_m)^{-1}$ for high values of IT_L. The inversion effect shows that light-induced optical coherence between the states $|a\rangle$ and $|b\rangle$ works against the process driving the molecule from $|b\rangle$ to $|c\rangle$. Obviously, the interaction causing the transition $|b\rangle \to |c\rangle$ does not affect optical coherence and is most likely a non-electromagnetic interaction affecting primarily the nuclear dynamics in the molecule. In Ref. [2], the transition $|b\rangle \to |c\rangle$ is described by a decay process. A more consistent description uses a time-asymmetric evolu-

tion in the optically excited molecule [6].

The time constant $\tau_R \approx 40$ μs measured by radiative decay [5] or with use of the Hanle effect [1], agrees well with results of optical radio-frequency double resonance experiments (see Ref. [7] and references given there), and with results of "time of flight" experiments (see Ref. [8] and Sec. 2 below). The time constant τ_0 was extracted from the width of the "broad" Hanle signal (Ref. [1]), from the width of the "broad rf-resonance" (see Refs. [6] [9] and Sec. 2), and from the width of the "ν-resonance" (see Ref. [8] and Sec. 2). The time constant τ_0 agrees also with the lifetime τ_{in} evaluated with use of the integrated absorption coefficient giving values for τ_{in} between 1 μs and 4 μs (Ref. [10] and references given there). In general, one expects $\tau_{in} = \tau_R$. The disagreement of τ_{in} with τ_R by more than a factor 10 was assigned to a coupling of levels of the first excited electronic state A^2B_2 with high lying vibrational levels of the ground electronic state and τ_{in} was identified with the lifetime of the uncoupled A^2B_2 electronic state [11] [12]. This theory is not in agreement with the occurrence of two time constants τ_0 and τ_R simultaneously on a single isolated hfs-level of NO_2. Moreover, radiative decay with the time constant τ_{in} was never detected by optical excitation near $\lambda_{ex} =$ 593 nm [5] [10]. In this work, we identify τ_{in} with τ_0 and give a different interpretation of the disagreement of τ_{in} with τ_R.

The present work aims to explain the transition $|b\rangle \to |c\rangle$ and the time constant τ_0 We have experimental evidence (see Ref. [13] and Sec. 2 of this work) that the transition $|b\rangle \to |c\rangle$ with the time constant τ_0 and with the associated inversion effect is a property of the isolated hfs-levels of NO_2 and is not due to collisions with baryonic matter or due to an intrinsic (intramolecular) process in the molecule. We give a phenomenological description of the experimental results based on the following assumption: The molecule interacts by gravity with a background field, presumably the axion dark matter field (e.g. Refs. [14] [15] [16] [17]), and based on ADD-theory (see Refs. [18] [19]), gravity is strong in a compactification space of the size of the molecule. Most investigations of axion effects on atoms and molecules focus on non-gravitational interactions (e.g. Refs. [14] [15] [16]). However, gravitational interaction may become strong, if one assumes, as in ADD-theory, that the three forces of the standard model act in three dimensions, but gravity acts in a higher $(3 + n_e)$-dimensional space, where n_e refers to the number of extra dimensions [18] [19]. Axions are an essential ingredient of various compactification scenarios including string theory and other theories with nontrivial extra dimensions (e.g. Refs. [20] [21] [22] [23]). Our proposal is as follows. In $|a\rangle$, all nuclei of NO_2 are completely confined in a single compactification space, and in $|c\rangle$, the two O nuclei of NO_2 are in two different compactification spaces. Whereas $|a\rangle$ and $|c\rangle$ represent stable configurations of the nuclei, $|b\rangle$ represents an unstable configuration because the vibrational motion in $|b\rangle$ shifts one of the two O nuclei periodically off the common compactification space, enabling the dark matter field to stimulate the transition $|b\rangle \to |c\rangle$ with the rate $(\tau_0)^{-1}$. In Sec. 2, we revisit experimental re-

sults, which were not understood before, and in Sec. 3 we discuss these results. Finally, in Sec. 4 we present our conclusion based on these results.

2. Experimental Results Revisited

We discuss experimental results, which were described in detail in Refs. [8] [9]. **Figure 1** depicts schematically the experimental arrangement. NO_2 molecules are propagating freely in an effusive molecular beam along the z-axis. A 50% beam splitter splits the light beam of a single mode cw laser (spectral width < 10 MHz) into two beams L_1 and L_2, which both cross the molecular beam. L_1 and L_2 have the same linear polarization parallel to the z-axis (π-excitation). The angle α can be varied continuously around $\alpha = 0$. For $\alpha = 0$ both light beams are parallel to each other (at right angle to the z-axis) and are separated by the gap width s. The gap width s as well as the aperture width d are both adjustable in the experiments. Here, d determines the diameters of L_1 and L_2.

Both s and d define the time of flight ($T_s + T_L$) of the molecules from the centre of L_1 to the centre of L_2 with $s = uT_s$ and $d = uT_L$. Here T_L is the transit-time of the molecules through L_1 or L_2. If ν is the light frequency as seen by the molecules in L_1, the molecules in L_2 see $\nu + \delta\nu$ with $\delta\nu = \nu\alpha(u/c)$ for small α. Here $u = 610 \pm 25\ \mathrm{ms}^{-1}$ is the average velocity of the molecules along the z-axis and c the velocity of light. The measured quantity is $A = (P - P_o)/P_o$ either versus the angle α or (with $\alpha = 0$) versus a magnetic field B, which is parallel to the z-axis. Here P is the fluorescence intensity as seen by a photomultiplier (perpendicular to the z-axis) and $P = P_o$ if α or B is off-resonance at a well-defined value. In the experiments, the laser light is tuned (with $\alpha = 0$) to a molecular transition near $\lambda_{ex} = 593$ nm. Then the beam divergence of L_1 and L_2 is adjusted to a maximum parallel light beam (flat wave surface at the intersection with the molecular beam). This adjustment seems to provide a maximum of optical coherence between $|a\rangle$ and $|b\rangle$ during T_L and has a strong effect on the fluorescence intensity P. Depending on T_L, this adjustment reduces P up to 50% of the P value for strongly focused L_1 *and* L_2 at constant laser power [8]. This

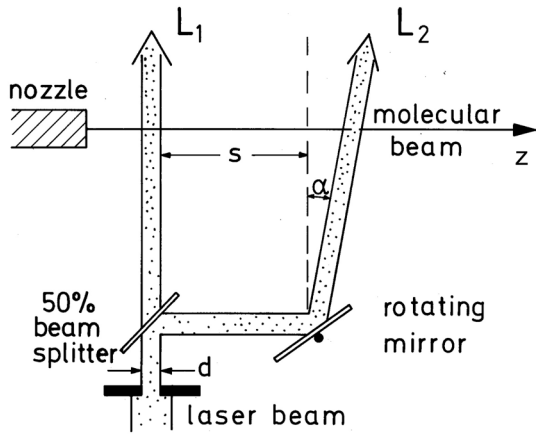

Figure 1. Schematic diagram of the experimental apparatus enabling experiments in the arrangements S_1, S_2, and S_3 (see text).

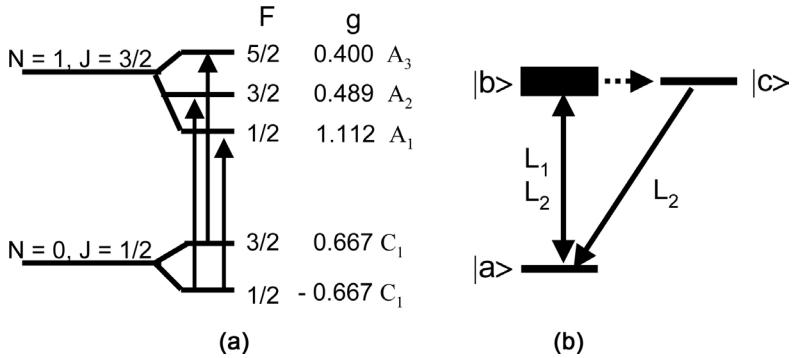

Figure 2. (a) Laser induced transitions (λ^{-1} = 16850.29 cm^{-1}) between hfs-levels (F, g-factor) of the ground state fs-level ($N = 0$, $J = 1/2$) and the excited state fs-level ($N = 1$, $J = 3/2$). (b) Each optical transition between a single hfs-level in the ground state and a single hfs-level in the excited state comprises the states $|a\rangle$, $|b\rangle$, and $|c\rangle$.

property of the optical excitation process is an essential ingredient to the experiments on NO_2 discussed here and was never reported for another molecule to the knowledge of the author.

The residual Doppler width in the molecular beam is about 50 MHz. The laser light induces a transition between a well-defined fine structure (fs) level in the ground state and a well-defined fs-level in the excited state. We investigated up to 20 such absorption lines in NO_2. **Figure 2(a)** depicts the transition between the ground state fs-level ($N = 0$, $J = 1/2$) and the excited state fs-level ($N = 1$, $J = 3/2$). The level structure is represented by the angular momentum coupling schema $N + S = J$ and $J + I = F$, where N, S, I, and F are the rotational, electron spin, nuclear spin and total angular momentum quantum numbers of the predominant isotopic form $^{14}N^{16}O_2$. The ^{14}N nucleus has $I = 1$ and the ^{16}O nucleus has $I = 0$. The hyperfine structure (hfs) splitting in the ground and excited state is larger than 5 MHz (see discussion in Refs. [8] [9]) and the excitation width of the laser light is less than 0.2 MHz (see below). Consequently, the laser light induces in a molecule a transition between a single hfs-level in the ground state and a single hfs-level in the excited state. **Figure 2(a)** depicts possible transitions ($\Delta F = +1$ and $\Delta F = 0$). We will show that each such transition between an hfs-level in the ground state and an hfs-level in the excited state comprises the states $|a\rangle$, $|b\rangle$, and $|c\rangle$ as depicted in **Figure 2(b)** and described above.

We used the experimental apparatus depicted in **Figure 1** in three different arrangements designated S_1, S_2, and S_3 in the following. In S_1, the angle α is fixed at $\alpha = 0$ and the molecules interact with a static magnetic field B parallel to the z-axis and with a radio-frequency (rf) field having constant frequency and linear polarization perpendicular to the z-axis. The measured quantity is $A = (P - P_o)/P_o$ versus B. **Figure 3** depicts the measured resonance spectrum with A_1, A_2, A_3, and C_1 indicating magnetic field values corresponding to the g-factors given in **Figure 2(a)**, which were known before e.g. by optical-rf double resonance experiments (see discussion in Refs. [8] [9]). The narrow resonances in **Figure 3** appear on top of a broad resonance structure, which we discuss in the next paragraph. The

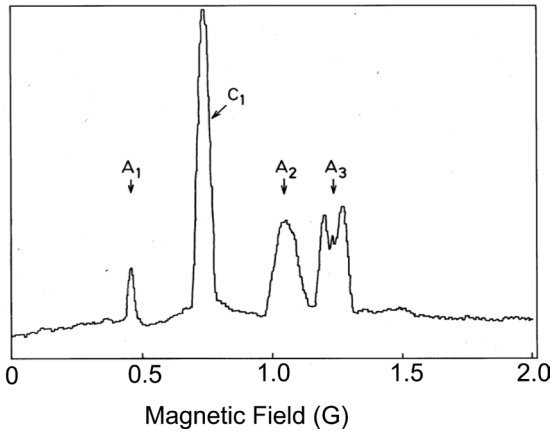

Figure 3. Magnetic resonance spectrum using the set-up S_1 with A_1, A_2, A_3, und C_1 indicating expected magnetic resonances corresponding to the g-factors in **Figure 2(a)**. The y-axis represents the quantity $A=(P-P_0)/P_0$ (see text). The Figure is taken from Ref. [8].

narrow resonances (but not the broad resonance structure) disappear if we use only L_1 or only L_2. The perturbation (due to optical-rf double resonance, see discussion in Ref. [8]) appearing on top of the resonance at A_3 exists also if we use eithe*r* L_1 *or* L_2 solely. The narrow resonances in **Figure 3** are assigned to molecules being either in $|a\rangle$ or in $|c\rangle$. L_1 depopulates some $|a,m\rangle$ and populates the linked $|b,m\rangle$, which evolve fast into the $|c,m\rangle$ (see **Figure 2(b)**). During the time of flight (T_s + T_L) the rf-field induces $\Delta m = \pm 1$ transitions in the $|a,m\rangle$ and $|c,m\rangle$, which are detected by L_2 causing an increase (by about 1%) of the fluorescence intensity P. (The rf-transitions in $|b\rangle$ contribute to the broad resonance structure.) The technique is well known (e.g. [24]). Measurements of the width ΔB of the narrow resonances versus the time of flight (T_s + T_L) give $\Delta B = w_1(T_s+T_L)^{-1}$, where w_1 is a constant comprising the Planck constant, the Bohr magnetron, the g-factor, and a numerical factor [8]. The width ΔB depends only on the apparative time constants and approaches zero for large values (T_s + T_L). The ratio of the signal strengths of resonances in $|c\rangle$ and in $|a\rangle$ versus (T_s + T_L) gives the lifetime τ_R = 40 ± 10 μs of $|c\rangle$ independent of constraints in the detection geometry (see below). These measurements show that the resonances are not affected by collisions during the time of flight measured up to (T_s + T_L) = 35 μs. This verifies that the molecules travel collision-free in the molecular beam.

There is a broad and unresolved resonance structure underlying the narrow resonances in **Figure 3**. This resonance structure can be resolved if T_L is increased. We used arrangement S_2, which is the same as S_1 but using L_1 only (L_2 is off). **Figure 4** depicts a result obtained in S_2 with T_L = 5.7 μs, whereas in **Figure 3** we used T_L = 1.6 μs. There are five Lorentzian shaped resonances associated with the same g-factors as in **Figure 3**. These resonances (an increase of P up to 5%) were named "broad rf-resonances" [6] [9]. These resonances are connected with the inversion effect [6]. The strength of these resonances depends strongly

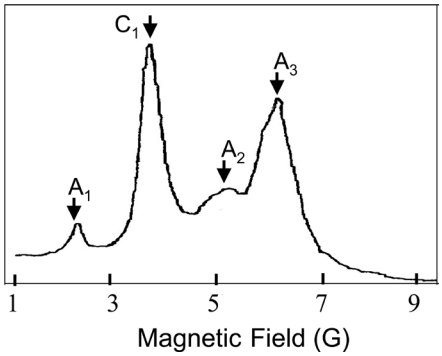

Figure 4. Magnetic resonance spectrum using the set-up S_2 with A_1, A_2, A_3, und C_1 indicating expected magnetic resonances corresponding to the g-factors in **Figure 2(a)**. The y-axis represents the quantity $A=(P-P_0)/P_0$ (see text).

on the adjustment of the divergence of L_1 as described above. These resonances enable measurements of the time constant τ_0 by the width of each resonance (after extrapolation of $(T_L)^{-1} \to 0$) and by the dependence of the signal strength of these resonances versus T_L [9]. The measurements of the "broad rf-resonances" are hampered by a compromise between nonlinearity of the Zeeman splitting and attainable resolution in the resonance spectrum. The width of the resonance at A_3 is already strongly affected by the nonlinear Zeeman splitting. Moreover, this resonance is also perturbed by an optical-rf double resonance signal similar to the resonance at A_3 in **Figure 3**. Taking these constraints into account, all resonances have the same properties in particular the same time constant $\tau_0 \approx 3$ µs as detailed investigations showed.

Figure 5 depicts the result of an α-scanning experiment using the set-up depicted in **Figure 1** in the arrangement S_3, *i.e.* using L_1 and L_2, but no rf-field and no static magnetic field B (the earth magnetic field is compensated). The measured quantity is $A=(P-P_0)/P_0$ versus $\delta\nu=\nu\alpha(u/c)$ with $P = P_0$ if α is far off-resonance. The signal is a change (up to 20%) of the fluorescence intensity P with a minimum at $\alpha = 0$ or $\delta\nu = 0$. It was named "ν-resonance" [8]. The signal shape is not Lorentzian but approximately Gaussian with the width (FWHM) $\Delta\nu$ and the amplitude A_ν. The result is $\Delta\nu=\Delta\nu_0+\Delta\nu_t+\Delta\nu_j$ with $\Delta\nu_0=(0.13\pm0.05)\,\text{MHz}$, with the transit time broadening $\Delta\nu_t=(0.87\pm0.05)(T_L)^{-1}$, and with $\Delta\nu_j=(7.6\pm1.0)\times10^9(T_s+T_L)(\text{Hz})^2$ being a contribution to the width $\Delta\nu$ due to laser frequency jitter during the time of flight ($T_s + T_L$). We have $\Delta\nu_0=(\pi\tau_0)^{-1}=0.13\,\text{MHz}$ with $\tau_0 = 2.5$ µs. The width $\Delta\nu$ is independent of the light intensity although the amplitude A_ν shows strong saturation versus the light intensity. Measurements of A_ν versus the time of flight ($T_s + T_L$) yield $A_\nu \sim \exp\left[-(T_s+T_L)(\tau)^{-1}\right]$ with $\tau = 22$ µs. The discrepancy between τ and $\tau_R \approx 40$ µs was attributed to the change of the detection geometry when the gap width s was varied but the photodetector was fixed. The analysis of this geometrical constraint showed that τ should be increased by at least 30% yielding $\tau \approx \tau_R$ (for details see Ref. [8]). We note that the recorded "ν-resonance" signals have generally an oblique underground which is connected

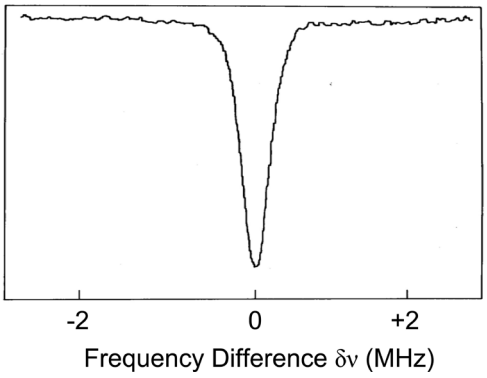

Figure 5. The y-axis represents the quantity $A=(P-P_0)/P_0$ (see text) measured in the set-up S_3 versus $\delta\nu=\nu\alpha(u/c)$. This signal is named "ν-resonance" in the text. The Figure is taken from Ref. [8].

with the angle tuning of the light beam L_2. This underground is also present without L_1. The underground (a straight line) is subtracted in the result shown in **Figure 5**.

3. Discussion

Figure 3 and **Figure 4** show that the g-factors enable an assignment of the measured data to the three excited hfs-levels depicted in **Figure 2(a)**. The experiments in arrangement S_1 (e.g. **Figure 3**) reveal that each hfs-level has a state $|c\rangle$ with the radiative lifetime $\tau_R \approx 40$ μs, and the experiments in arrangement S_2 (e.g. **Figure 4**) reveal that each hfs-level has a state $|b\rangle$ with the decay time $\tau_0 \approx 3$ μs. Moreover, a molecule evolves from $|b\rangle$ into one state $|c\rangle$ only and not into a bunch of states $|c\rangle$. The resonances in **Figure 3** disagree with a molecule being in a superposition of several states $|c\rangle$, because rf-transitions between different states $|c\rangle$ result in additional resonances and a broadening of the width. The assumption of a molecule being in a superposition of several states $|c\rangle$ disagrees also with the results of Hanle experiments and Zeeman quantum beat experiments, which both reveal a coherence decay time of $|c\rangle$ in agreement with the radiative lifetime τ_R [1] [25]. Evidently, the transition $|b\rangle \to |c\rangle$ transfers Zeeman coherence in the magnetic sublevels from a single state $|b\rangle$ to a single state $|c\rangle$. Therefore, the transition $|b\rangle \to |c\rangle$ is no intrinsic (intramolecular) process in the molecule, because there is no "sink" in the molecule to provide a recurrence time longer than the radiative lifetime [26]. We conclude that the level scheme (comprising the states $|a\rangle$, $|b\rangle$, and $|c\rangle$) depicted in **Figure 2(b)**, applies to all transitions in **Figure 2(a)** between an hfs-level in the ground state and an hfs-level in the excited state. Moreover, the perturbation causing the transition $|b\rangle \to |c\rangle$ is neither an intrinsic process in the molecule nor caused by baryonic matter collisions.

The "ν-resonance" in **Figure 5**, is a superposition of at least three signals, of which each one is associated with the excitation of one of the three hfs-levels in **Figure 2(a)**. Each signal is centred at $\delta\nu = 0$ with the same width

$\Delta\nu_0 = (\pi\tau_0)^{-1} = 0.13\,\text{MHz}$, with the same dependence on the transit-time T_L, and with the same time of flight ($T_s + T_L$). Therefore, the "ν-resonance" has the same properties as the corresponding signal in a single transition between an hfs-level in the ground state and an hfs-level in the excited state. The amplitude of the "ν-resonance" versus the time of flight ($T_s + T_L$) is $A_\nu \sim \exp\left[-(T_s + T_L)(\tau_R)^{-1}\right]$, if we assume $\tau = \tau_R$ taking into account the constraints in the detection geometry (see Sec. 2). A change of the population in $|a\rangle$ ("hole burning") does not affect A_ν in a detectable way. This result shows that the "ν-resonance" is predominantly due to induced emission from $|c\rangle$ to $|a\rangle$ as indicated in **Figure 2(b)**. However, there is no absorption process from $|a\rangle$ to $|c\rangle$. Light absorption from $|a\rangle$ to $|c\rangle$ contradicts the experimental results, in particular the inversion effect. What does it mean that $|b\rangle$ and $|c\rangle$ are both connected to $|a\rangle$ by an electric-dipole transition, but a molecule being in $|a\rangle$ is only excited into $|b\rangle$ by an optical transition? We conclude that the states $|a\rangle$ and $|b\rangle$ but not the state $|c\rangle$ are eigenstates of the hamiltonian H_{mol} of the unperturbed (no transition $|b\rangle \to |c\rangle$) molecule. In the unperturbed molecule, there is no state $|c\rangle$ and the state $|b\rangle$ has the decay rate $(\tau_R)^{-1}$. This conclusion disproves the proposal in Ref. [13]. The perturbation causing the transition $|b\rangle \to |c\rangle$ affects the molecule in $|b\rangle$ and modifies $|b\rangle$ into $|c\rangle$ with the rate $(\tau_0)^{-1}$ without changing the radiative decay rate significantly. The two "states" $|b\rangle$ and $|c\rangle$ represent a substructure of a single isolated hfs-level of the molecule.

The level width of $|b\rangle$ represented e.g. by the width of the "broad rf-resonance" or by the width $\Delta\nu_0 = (\pi\tau_0)^{-1} \approx 100\,\text{kHz}$ of the "ν-resonance" corresponds to an energy spread of about 400 peV. This width is by a factor of about $\tau_R(\tau_0)^{-1} \geq 10$ larger than the natural linewidth $(2\pi\tau_R)^{-1} \approx 4$ kHz of $|c\rangle$. A molecule evolves from $|b\rangle$ into a single state $|c\rangle$. However, the level energy of $|c\rangle$ seems to vary within the width of $|b\rangle$. We assign the near Gaussian shape of the "ν-resonance" to the distribution of the level energies of $|c\rangle$ within the width of $|b\rangle$ in the ensemble of excited molecules. The level energies of $|c\rangle$ are no eigenvalues the usual molecular hamiltonian of an isolated molecule. A complete description of the molecule requires to take account of the perturbation causing the transition $|b\rangle \to |c\rangle$. The level energies of $|c\rangle$ seem to occupy an energy band having a width determined by the decay rate $(\tau_0)^{-1}$ and representing an effective degeneracy $g_u \approx \tau_R(\tau_0)^{-1}$ of the excited hfs-level. A molecule is only in one of these $|c\rangle$ levels.

An effective degeneracy $g_u \approx \tau_R(\tau_0)^{-1}$ of the excited hfs-levels explains the difference between the lifetime τ_R measured by radiative decay measurements and the lifetime τ_{in} measured by the integrated absorption coefficient [10] [11]. According to Equation (22) of Ref. [27], τ_{in} is given by $\tau_{in} = (g_u/g_l)A_{in}$, where the quantity A_{in} includes an integral over the whole of the absorption band concerned, and g_l and g_u are the degeneracy of the lower (l) and the upper (u) state involved, respectively. In Refs. [10] [11], τ_{in} was evaluated using $g_l = g_u = 1$,

which gives $\tau_{in} = A_{in} \approx 3\,\mu\text{s} \approx \tau_0$. However, assuming an effective degeneracy $g_u \approx \tau_R(\tau_0)^{-1}$ of the excited hfs-level and $g_l = 1$, we obtain $\tau_{in} = \left[\tau_R(\tau_0)^{-1}\right] A_{in} = \tau_R$ with $A_{in} = \tau_0$. This result eliminates the discrepancy between the radiative lifetime τ_R and the lifetime τ_{in} evaluated on the basis of the integrated absorption coefficient. Finally, we note that a disagreement between τ_{in} and τ_R is also known for the molecules SO_2 and CS_2 [11] [12].

In $|a\rangle$, the molecule is in the vibrational ground state with no vibrational mode excited. The vibrational quantum numbers of $|b\rangle$ and $|c\rangle$ are not known. Spectroscopic studies (near $\lambda_{ex} = 593$ nm) on a static NO_2 gas sample (50 mTorr) suggest totally symmetric vibrational symmetry (no asymmetric stretch mode excited) of the excited state establishing the A^2B_2 electronic symmetry for this state (see Ref. [28] and a similar result in Ref. [29]). These studies reveal also that the N-O bond length is significantly longer in $|b\rangle$ than in $|a\rangle$ [28]. However, the strongly collision disturbed fluorescence spectrum favours the study of $|b\rangle$ only and gives no information on $|c\rangle$. The experiments in Refs. [1] [2] show that $|b\rangle$ and $|c\rangle$ differ in the degree of polarization of the fluorescence light. In Ref. [2], we conclude that $|b\rangle$ has a symmetric configuration (equal N-O bond lengths) in agreement with the results in Ref. [28], whereas $|c\rangle$ has an asymmetric configuration (unequal N-O bond lengths). In Ref. [2], we associate $|c\rangle$ with a state having its energy minimum at linearity of the O-N-O angle and a strong asymmetry in the N-O bond length [30].

What causes the transition $|b\rangle \to |c\rangle$? As already noted, we are able to exclude collisions with baryonic matter and an intrinsic (intramolecular) process in the molecule. The inversion effect shows that optical coherence between $|a\rangle$ and $|b\rangle$ works against the transition $|b\rangle \to |c\rangle$. Therefore, we conclude that the perturbation causing this transition affects the molecule in $|b\rangle$ but not in $|a\rangle$, and it does not affect optical coherence. As optical coherence is fast perturbed by electromagnetic interaction, we assume a non-electromagnetic interaction affecting primarily the nuclear dynamics in the molecule. However, a change e.g. in the N-O bond length affects easily also electronic dynamics in the excited molecule, because the potential energy surfaces of several electronic states (e.g. X^2A_1, A^2B_2, and B^2B_1 in C_{2v} symmetry) are degenerate (intersect) and coupled e.g. by the antisymmetric stretch vibration mode (e.g. [31] [32] [33] and references given there). Therefore, also small perturbations of the nuclear configuration affect the symmetry of the electronic state and are thus enhanced to an optically detectable signal.

4. Conclusion

Experiments on NO_2 reveal a substructure underlying the isolated hyperfine structure (hfs) levels of the collision-free, optically excited molecule. This substructure is seen in a change of the symmetry of the excited molecule and is represented by the two "states" $|b\rangle$ and $|c\rangle$ underlying a single hfs-level. This finding contradicts our expectation on a molecule being excited into a stationary

state of the usual molecular hamiltonian. We propose the following interpretation of the experimental results. The molecule interacts by gravity with a background dark matter field, presumably the axion dark matter field, and, based on ADD-theory [18] [19], gravity is strong in a compactification space of the size of the molecule. The first assumption implies identifying the decay rate $(\tau_0)^{-1}$ with the oscillation frequency of the axion field (e.g. [14] [15]). This gives $mc^2 \approx 200$ peV for the mass m of the axion. In applying the second assumption, we note that the N-O bond lengths differ in $|a\rangle$, $|b\rangle$, and $|c\rangle$ with $|a\rangle$ having the shortest and $|c\rangle$ having the longest bond length. We propose the following. In $|a\rangle$, all nuclei of NO_2 are completely confined in a single compactification space, and in $|c\rangle$, the two O nuclei are in two different compactification spaces. At the shorter bond length N-O, the N and O nuclei are confined in one compactification space, and at the longer bond length N-O, the O nucleus is isolated in a separate compactification space. We do not exclude a tunneling motion between the two configurations of an O nucleus. The experiments show that $|a\rangle$ and $|c\rangle$ represent stable configurations of the nuclei, whereas $|b\rangle$ is an unstable configuration of the nuclei. Here "stable" means that the dark matter field does not affect the configuration of the nuclei. In $|b\rangle$ the configuration of the nuclei is unstable, because presumably the vibrational motion shifts one of the two O nuclei periodically off the common compactification space. This enables the axion field to stimulate the transition $|b\rangle \to |c\rangle$ with the rate $(\tau_0)^{-1}$. A coherent superposition of $|b\rangle$ and $|a\rangle$ reduces this action of the axion field, because this field does not affect the molecule in $|a\rangle$. This explains the inversion effect. Moreover, molecule and axion field are a non-separable system with an effective degeneracy of about $\tau_R\,(\tau_0)^{-1}$ of the excited hfs-levels. This explains the difference between the lifetime τ_R measured by radiative decay measurements and the lifetime τ_{in} measured by the integrated absorption coefficient. The phenomenological description given here does not explain the dynamics of the transition $|b\rangle \to |c\rangle$. This is beyond the scope of the experimental work reported here and needs further clarification by theory.

Acknowledgements

This work is dedicated to my friend and colleague Dr. Franciszek Bylicki, Torun, Poland, who died in 2016. He contributed much to the experimental work reported here.

References

[1] Weber, H.G. (1988) *Physical Letters A*, **129**, 355. https://doi.org/10.1016/0375-9601(88)90001-1

[2] Weber, H.G. (2015) *Physical Letters A*, **379**, 1342. https://doi.org/10.1016/j.physleta.2015.03.008

[3] Sanrey, M. and Joyeux, M. (2007) *The Journal of Chemical Physics*, **126**, 074301. https://doi.org/10.1063/1.2446920

[4] Ruf, H., *et al.* (2012) *The Journal of Chemical Physics*, **137**, 224303. https://doi.org/10.1063/1.4768810

[5] Cheshnovsky, O. and Amirav, A. (1984) *Chemical Physics Letters*, **109**, 368. https://doi.org/10.1016/0009-2614(84)85603-1

[6] Weber, H.G. (1985) *Physical Review A*, **31**, 1488. https://doi.org/10.1103/PhysRevA.31.1488

[7] Bylicki, F., Weber, H.G., Zscheeg, H. and Arnold, M. (1984) *The Journal of Chemical Physics*, **80**, 1791. https://doi.org/10.1063/1.446936

[8] Weber, H.G. (1986) *Zeitschrift für Physik D Atoms, Molecules and Clusters*, **1**, 403. https://doi.org/10.1007/BF01431183

[9] Weber, H.G. and Miksch, G. (1985) *Physical Review A*, **31**, 1477. https://doi.org/10.1103/PhysRevA.31.1477

[10] Donnelly, V.M. and Kaufman, F. (1978) *The Journal of Chemical Physics*, **69**, 1456. https://doi.org/10.1063/1.436770

[11] Douglas, A.E. (1966) *The Journal of Chemical Physics*, **45**, 1007. https://doi.org/10.1063/1.1727650

[12] Bixon, M. and Jortner, J. (1969) *The Journal of Chemical Physics*, **50**, 3284. https://doi.org/10.1063/1.1671552

[13] Weber, H.G. (2015) *Chemical Physics Letters*, **639**, 243.

[14] Graham, P.W. and Rajendran, S. (2011) *Physical Review D*, **84**, Article ID: 055013. https://doi.org/10.1103/PhysRevD.84.055013

[15] Roberts, B.M., Stadnik, Y.V., Dzuba, V.A., Flambaum, V.V., Leefer, N. and Budker, D. (2014) *Physical Review D*, **90**, Article ID: 096005. https://doi.org/10.1103/PhysRevD.90.096005

[16] Vavra, J. (2014) *Physics Letters B*, **736**, 169.

[17] Borsanyi, S., *et al.* (2016) *Nature*, **539**, 69-71. https://doi.org/10.1038/nature20115

[18] Arkani-Hamed, N., Dimopoulos, S. and Dvali, G. (1998) *Physics Letters B*, **429**, 263-272.

[19] Antoniadis, I., Arkani-Hamed, N., Dimopoulos, S. and Dvali, G. (1998) *Physics Letters B*, **436**, 257.

[20] Svrcek, P. and Witten, E. (2006) *JHEP*, **0606**, 051.

[21] Ringwald, A. (2014) *Journal of Physics: Conference Series*, **485**, Article ID: 012013. https://doi.org/10.1088/1742-6596/485/1/012013

[22] Dienes, K.R., Dudas, E. and Gherghetta, T. (2000) *Physical Review D*, **62**, Article ID: 105023. https://doi.org/10.1103/PhysRevD.62.105023

[23] Kribs, G.D. (2006) TASI 2004 Lectures on the Phenomenology of Extra Dimensions.

[24] Rosner, S.D., Holt, R.H. and Gaily, T.D. (1975) *Physical Review Letters*, **35**, 785. https://doi.org/10.1103/PhysRevLett.35.785

[25] Brucat, P.J. and Zare, R.N. (1983) *The Journal of Chemical Physics*, **78**, 100. https://doi.org/10.1063/1.444529

[26] Bixon, M. and Jortner, J. (1968) *The Journal of Chemical Physics*, **48**, 715. https://doi.org/10.1063/1.1668703

[27] Strickler, S.J. and Berg, R.A. (1962) *The Journal of Chemical Physics*, **37**, 814. https://doi.org/10.1063/1.1733166

[28] Stevens, C.G. and Zare, R.N. (1975) *Journal of Molecular Spectroscopy*, **56**, 167.

[29] Brand, J.C.D., Hardwick, J.L., Pirkle, R.J. and Seliskar, C.J. (1973) *Canadian Journal of Physics*, **51**, 2184. https://doi.org/10.1139/p73-284

[30] Schinke, R. (2008) *The Journal of Chemical Physics*, **129**, Article ID: 124303. https://doi.org/10.1063/1.2977597

[31] Ma, J., Liu, P., Zhang, M. and Dai, H.-L. (2005) *The Journal of Chemical Physics*, **123**, Article ID: 154306. https://doi.org/10.1063/1.2049271

[32] Arasaki, Y., Takatsuka, K., Wang, K. and McKoy, V. (2010) *The Journal of Chemical Physics*, **132**, Article ID: 124307. https://doi.org/10.1063/1.3369647

[33] Sardar, S., Mukherjee, S., Paul, A.K. and Adhikari, S. (2013) *Chemical Physics*, **416**, 11.